J. Biochem. **121**, 1076-1081 (1997)

Analysis of the Stabilization of Hen Lysozyme by Helix Macrodipole and Charged Side Chain Interaction

Hiroyuki Motoshima, Shouhei Mine, Kiyonari Masumoto, Yoshito Abe, Hiroki Iwashita, Yoshio Hashimoto, Yuki Chijiiwa, Tadashi Ueda, and Taiji Imoto[1]

Graduate School of Pharmaceutical Sciences, Kyushu University 62, Maidashi, Higashi-ku, Fukuoka 812-82

Received for publication, December 24, 1996

In the N-terminal region of the α-helix of the c-type lysozymes, two Asx residues exist at the 18th and 27th positions. Hen lysozyme has Asp18/Asn27 (18D/27N), and we prepared three mutant lysozymes, Asn18/Asn27 (18N/27N), Asn18/Asp27 (18N/27D), and Asp18/Asp27 (18D/27D). The stability of the wild-type (18D/27N) lysozyme supported the existence of a hydrogen bond between the side chain of Asp18 and the amide group at the N1 position in the α-helix, while the stability of the 18N/27D lysozyme supported the presence of the capping box between the Ser24 (N-cap) and Asp27 residues. Although electrostatic repulsion was observed between Asp18 and Asp27 residues in 18D/27D lysozyme, the dissociation of each residue contributed to stabilizing the B-helix in 18D/27D lysozyme through hydrogen bonding and charge-helix macrodipole interaction. This is the first evidence that two neighboring negative charges at the N-terminus of the helix both increased the stability of the protein.

Key words: hen lysozyme, NMR, site-directed mutagenesis, stability, X-ray crystallography.

A degree of instability of proteins is important for physiological reasons, such as turnover. However, when proteins are to be used as drugs, catalysts, and so on, it is desirable to improve their stability. The α-helix has 3.6 residues per turn and a translation per residue of 1.5 Å. It can be divided into three regions, the N-terminal region, the helix center, and the C-terminal region. The main chain atoms of each amino acid unit in the helix center have two hydrogen bonds, while those in the N-terminal and the C-terminal regions have one hydrogen bond.

The helix has a dipole moment with the positive pole at the N-terminus and the negative one at the C-terminus (*1*). Based on crystallographic data, it has been reported that Asp and Glu residues exist in the N-terminal neighborhood of the α-helix and that Lys, Arg, and His residues exist in the C-terminal neighborhood of the α-helix (*2*). Therefore, electrostatic interaction between charges and the helix dipole should take part in the stabilization of a protein.

Several methods of stabilizing a protein by improving the interaction at the N-terminus or the C-terminus of the helix by means of one-point mutation have been reported. For example, the α-helix of a synthetic peptide was stabilized by introducing a charged residues at both ends (*3*). Barnase was stabilized by introducing a charged residue, His, at the C-terminus of the α-helix (*4, 5*) and the thermostabilization of T4-lysozyme was achieved by introducing the charged residue, Asp, at the N-terminus of the α-helix (*6*). On the other hand, there is no report that double charges at the N-terminus of the helix affect the stability of a protein, although it has been demonstrated that the instability of RNase T_1 is due to the presence of two charged residues, Glu and Asp, at the C-terminus of the α-helix (*7*).

In almost all of the c-type lysozymes, a surface-exposed acidic residue is located at position 18, near the N-terminus of the α-helix, which extends from residues 25 to 35 (B-helix). In rat, mouse-P, or mouse-M lysozyme, a buried acidic residue is present at position 27, which is located at the N3 position of the B-helix. Residues 18 and 27 in hen lysozyme are Asp and Asn, respectively (Table I and Fig. 1). To date, however, no data are available on the stability of rat and mouse lysozymes. Therefore, in this paper, we focus our attention on how the buried acidic residue at Asp27 contributes to the stability and how it affects the dissociable residue (Asp18) located near position 27, because the distance between the Cγ atoms of these residues is about 10 Å based on X-ray crystallographic data.

Thus, we prepared three mutant lysozymes, Asn18/Asn27 (18N/27N), Asn18/Asp27 (18N/27D), and Asp18/Asp27 (18D/27D), and compared their stability and structure with those of the wild-type lysozyme (18D/27N) using X-ray crystallography and NMR analysis.

MATERIALS AND METHODS

Materials—Restriction enzymes, T4 polynucleotide ki-

[1] To whom correspondence should be addressed.

Abbreviations: GdnHCl, guanidine hydrochloride; 18N/27N lysozyme, a mutant lysozyme in which Asp18 is mutated to Asn; 18D/27N lysozyme, wild-type lysozyme; 18N/27D lysozyme, a mutant lysozyme in which Asp18 and Asn27 are mutated to Asn and Asp, respectively; 18D/27D lysozyme, a mutant lysozyme in which Asn27 is mutated to Asp; DSS, 4,4-demethyl-4-silapentane-1-sulfonate; DQF-COSY, two-dimensional double-quantum-filtered J-correlated spectroscopy.

TABLE I. **Comparison of primary structure of hen, human, mouse P, mouse M, and rat lysozyme around the B-helix (25-35).**

	15 20 30 40	Reference
Hen	HGLDNYRGYSLGNWVCAAKFESNFNT	*21*
Human	L-MDG---I--AN-MCLA-W--GY--	*22*
Mouse P	N-MDG---VK-AD---L-QH--DY--	*23*
Mouse M	N-MAG-Y-V--AD---L-QH--DY--	*24*
Rat	N-MSG-Y-V--AD---L-QH--DY--	*25*
	B-helix	

nase, and DNA polymerase I (Klenow fragment) were purchased from either Takara Shuzo (Kyoto) or New England Biolabs (Beverly). *Micrococcus luteus* and DNA sequencing kits (Sequenase) were purchased from Sigma and Amersham Japan (Tokyo), respectively. CM-Toyopearl 650M, a cation-exchange resin for the purification of secreted hen lysozyme, was obtained from Tosoh (Tokyo). A Wakopak $_5C_{18}$ column (200 mesh) was obtained from the Wako Pure Chemicals Institute (Osaka). All other chemicals were of analytical grade for biochemical use.

Purification and Identification of Lysozymes Secreted by Yeast—Mutant lysozymes (18N/27N, 18N/27D, and 18D/27D lysozyme) were prepared as described before (*8*). Each yeast (*Saccharomyces cerevisiae* AH22) transformant was cultivated at 30°C for 125 h for expression and secretion of each lysozyme, as described before (*8*). Purification (ion-exchange chromatography) and identification (peptide mapping, amino acid sequencing, and amino acid composition) of the lysozymes secreted by the yeast were carried out as before (*9*). Each mutation was confirmed by DNA sequencing and peptide analysis (*9*).

Stability of Mutant Lysozymes Examined by GdnHCl Denaturation—Unfolding equilibria of the lysozymes in the presence of guanidine hydrochloride (GdnHCl) were evaluated at pH 5.5 and 35°C by measuring the fluorescence at 360 nm (excited at 280 nm). The protein concentration was 9.3×10^{-7} M, and the buffer used was 0.1 M sodium acetate adjusted to pH 5.5 with HCl. Details of the analysis were the same as described earlier (*9*). Namely, by assuming a two-state transition for unfolding, the equilibrium constant between the folded (N) and the unfolded (D) states, $K_D = D/N$, and the free energy of unfolding, $\Delta G = -RT\ln K_D$, at a given concentration of GdnHCl were calculated from each unfolding curve, and a least-squares analysis was used to fit the data to Eq. 1,

$$\Delta G = \Delta G(H_2O) - m[\text{GdnHCl}] \quad (1)$$

where $\Delta G(H_2O)$ is the value of ΔG in the absence of GdnHCl and m is a measure of the dependence of ΔG on GdnHCl concentration. The midpoint of GdnHCl denaturation is $C_{0.5} = \Delta G(H_2O)/m$, because $\Delta G = 0$ at $C_{0.5}$. The values of $\Delta\Delta G(H_2O)$ are calculated using Eq. 2 and the average m value of the wild-type and mutant lysozymes.

$$\Delta\Delta G(H_2O) = \Delta G(H_2O)_{\text{LYSOZYME}} - \Delta G(H_2O)_{\text{18N/27N}} \quad (2)$$

X-ray Crystallography of Mutant Lysozymes—Mutant lysozymes were crystallized from 50 mM sodium acetate at pH 4.7 containing 0.9-1.2 M NaCl; the conditions are the same as those for crystallization of native lysozyme (*10*). The crystal was grown by vapor diffusion using the hanging-drop method. Mutant lysozymes gave crystals isomorphous with those of the wild-type lysozyme (18D/27N lysozyme).

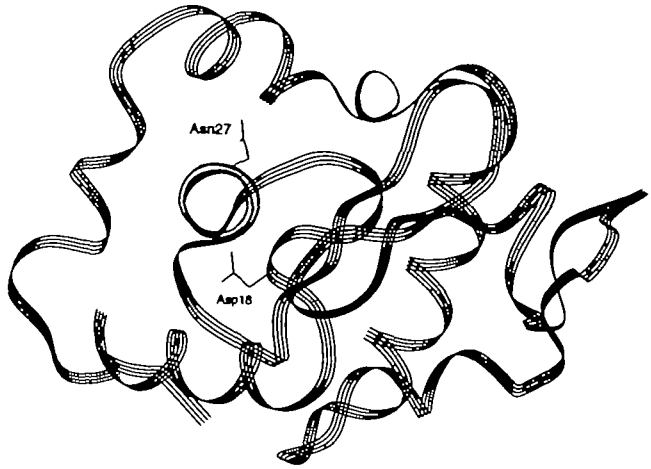

Fig. 1. **Ribbon drawing of the backbone conformation of hen lysozyme with the residues of interest.** Asp18 and Asn27 are located near the N-terminal end of the B-helix (25-35) in hen lysozyme.

The crystals belong to the tetragonal system, space group $P4_32_12$. The intensity data to below 2.0 Å were collected at room temperature on a Rigaku R-AXIS II C area detector using a Rigaku RU-300 rotating anode source operating at 40 kV and 120 mA. The intensity data were reduced using the Rigaku PROCESS software package. Because the mutant crystals were isomorphous to the wild-type crystal ($P4_32_12$, cell dimensions $a=b=79.21$, and $c=37.97$ Å), the coordinates of the wild-type were used as the starting model for the refinement. The structures of mutant lysozymes were refined using X-PLOR 3.1 (*11*). These structures were fitted to the Sim-weighted difference-electron density maps using the program package TURBO-FRODO 5.1 (*12*) on SGI indigo^2. The first refinements dropped the R-values of the mutant lysozymes below 23.0%. Water molecules were added and the next refinements were carried out. The final refinements of these structures including the water molecules gave R-values below 18.0%. The coordinates have been assigned ID codes in the Protein Data Bank as follows: wild-type, 1RFP; 18N/27N, 1KXW; 18N/27D, 1KXX; 18D/27D, 1KXY.

Measurement of ^{1}H-NMR—The lysozymes were dialyzed against the solution at the measuring pH; then D_2O and NaCl were added so that the protein was in solution in 90% H_2O:10% D_2O containing 5 mM NaCl. The pH values of the solution containing about 2 mM lysozyme were readjusted by adding dilute DCl or NaOD; the pH meter readings were not corrected for isotope effects (*13*). The probe temperature was calibrated with an accuracy of ±0.2°C using ethylene glycol. The uncertainty in the reported pH values arising from the temperature dependence, was within ±0.1 pH unit. All chemical shifts are obtained by reference to DSS. The deviation in the measured chemical shifts is ±0.02 ppm.

^{1}H-NMR experiments were performed on a Varain Unity 600 plus NMR spectrometer. Phase-sensitive DQF-COSY (*14*) and NOESY (*15*) experiments at pH 3.8 and 35°C were carried out at 600 MHz using the standard procedure except for pH titration. Typically 96 transients were recorded for each of 512 increments. A digital resolution of

5.8 Hz/point in both dimensions was used for both the COSY and NOESY spectra. The assignments of the signals were made by reference to the literature (*16*).

RESULTS

The Stability of Lysozymes Determined by GdnHCl Denaturation—In Table II, the values of $C_{0.5}$, $\Delta G(H_2O)$, and $\Delta\Delta G(H_2O)$ of the respective lysozymes as well as the m values are summarized. When the stability of each mutant lysozyme at pH 5.5 was compared with that of 18N/27N lysozyme, 18N/27D lysozyme was stabilized by 1.5 kJ/mol, 18D/27N lysozyme was stabilized by 2.3 kJ/mol, and 18D/27D lysozyme was stabilized by 3.8 kJ/mol.

Crystal Structures of Lysozymes—The crystallographic data collection and refinement statistics for crystal structures of the wild-type and mutant lysozymes are summarized in Table III. The refined structures of the mutant lysozymes were in good agreement with that of the wild-type lysozyme. Superimposing each mutant lysozyme on the wild-type lysozyme, we calculated the root mean square (r.m.s.) deviation in the coordinates of the main chains to be 0.09 Å for the 18N/27N lysozyme, 0.13 Å for the 18N/27D lysozyme, and 0.13 Å for the 18D/27D lysozyme.

(1) 18N/27N lysozyme: The N-terminal region of the B-helix in the 18N/27N lysozyme (thin line) is shown in Fig. 2A. The amide groups at the N1 and N2 positions in the B-helix in the 18N/27N lysozyme formed hydrogen bonds with two water molecules (WAT1 and WAT2). Namely, the amide group of Leu25 (N1) in the 18N/27N lysozyme did not form a hydrogen bond with the side chain of Asn18 because the electron density of the water's oxygen atom was clearly observed. The amide groups at the N3 and N4 positions did not form hydrogen bonds (Table IV).

(2) 18D/27N lysozyme (wild-type): The N-terminal

TABLE II. **Thermodynamic parameters characterizing the GdnHCl denaturation of mutant lysozymes at pH 5.5 and 35°C.**

Lysozyme	$C_{0.5}$ (M)	m (kJ/mol/M)	$\Delta G(H_2O)$[a] (kJ/mol)	$\Delta\Delta G(H_2O)$[b] (kJ/mol)
18N/27N	3.43±0.01	12.3	42.2	0
18D/27N (wild)	3.62±0.01	12.3	44.5	2.3
18N/27D	3.55±0.01	12.5	43.7	1.5
18D/27D	3.74±0.01	12.2	46.0	3.8

[a]The value was determined by using the mean value of m (12.3). [b]$\Delta\Delta G(H_2O)$ based on the 18N/27N lysozyme.

TABLE III. **Crystallographic data collection and refinement statistics of lysozymes.**

	18N/27N	18D/27N (wild)	18N/27D	18D/27D
Data collection				
Cell dimensions				
a,b (Å)	79.10	79.21	79.19	79.16
c (Å)	38.16	37.97	38.00	37.88
Resolution (Å)	1.79	1.75	1.71	1.95
Unique reflections $[F>1\sigma(F)]$	10,402	11,948	11,446	8,613
Completeness (%)	86.4	93.2	83.3	93.8
R-merge (%)[a]	7.74	3.69	6.82	4.70
Refinement				
R-factor (%)[b]	17.6	16.8	17.7	16.8
Δ bond length (Å)	0.010	0.009	0.010	0.009
Δ bond angle (°)	1.509	1.448	1.493	1.472
Number of water molecules	82	98	60	59

[a]R-merge $=\Sigma|F_i-F|/\Sigma F_i$, where F_i are repeated measurements of equivalent structure amplitudes and F is the average value of F_i. [b]R-factor $=\Sigma|F_{obs}-F_{calc}|/\Sigma F_{obs}$.

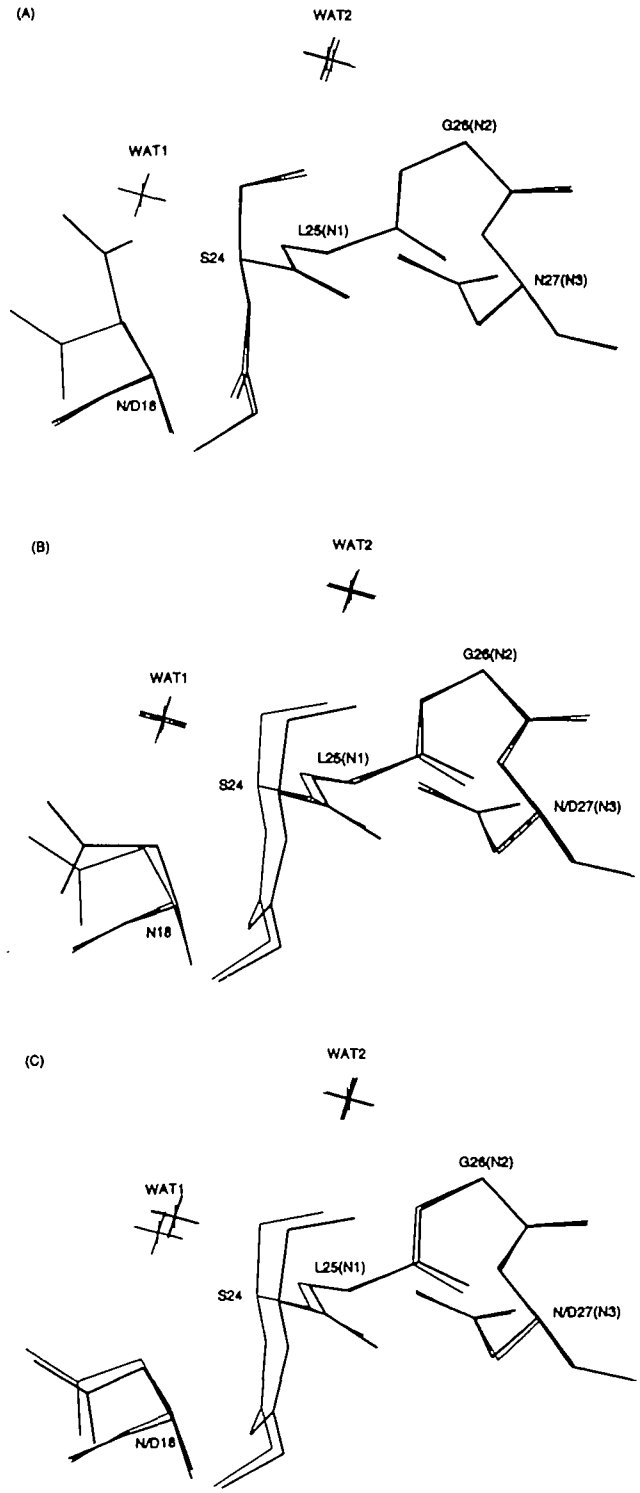

Fig. 2. **Superposition of the structure of each lysozyme (thick line) on that of 18N/27N lysozyme (thin line).** (A) is 18D/27N lysozyme (wild-type), (B) is 18N/27D lysozyme, (C) is 18D/27D lysozyme. The amide groups at the position of Leu25 (N1) and Gly26 (N2) form hydrogen bond with WAT1 and WAT2, respectively.

region of the B-helix in the 18D/27N lysozyme (wild-type, thick line) is shown in Fig. 2A. The amide groups at the N1 and N2 positions in the B-helix in the 18D/27N lysozyme formed hydrogen bonds with the side chain of Asp18 and a water molecule (WAT2), respectively. Moreover, the negative charge at Asp18 was located at a position where electrostatic interaction between the charge and the helix dipole in the B-helix could occur. The amide groups at the N3 and N4 positions did not form hydrogen bonds (Table IV).

(3) 18N/27D lysozyme: The N-terminal region of the B-helix in the 18N/27D lysozyme (thick line) is shown in Fig. 2B. The amide groups at the N1 and N2 positions in the B-helix in the 18N/27D lysozyme formed hydrogen bonds with two water molecules, like those in the 18N/27N lysozyme. A structural change at the N-cap position Ser24 in the B-helix was observed in the 18N/27D lysozyme due to the introduction of the negative charge at Asp27. Moreover, the amide groups at N3 and N4 positions formed hydrogen bonds with the hydroxyl group and the carbonyl group of Ser24, respectively. The distances between the atoms involved in Ser24 in the 18N/27D lysozyme are shown in Table IV. When we examined the hydrogen bond formation in both 18N/27N and 18N/27D lysozymes, an acceptor atom and a donor atom in the hydrogen bond were found to have changed. Therefore, the residue Ser24 at the N-cap position in the B-helix could form an end-capping structure in the 18N/27D lysozyme. Moreover, the amide groups at the N1, N2, N3, and N4 positions were confirmed to form hydrogen bonds.

(4) 18D/27D lysozyme: The N-terminal region of the B-helix in the 18D/27D lysozyme (thick line) is shown in Fig. 2C. A structural change at Ser24 in the 18D/27D lysozyme similar to that in the 18N/27D lysozyme was observed. The distances between atoms involved in Ser24 in the 18D/27D lysozyme are shown in Table IV. The hydrogen bonds involved in Ser24 in the 18D/27D lysozyme were identical to those of the 18N/27D lysozyme. Therefore, the residue Ser24 could form an end-capping structure in the 18D/27D lysozyme, and the amide groups at the N1, N2, N3, and N4 positions were confirmed to form hydrogen bonds. On the other hand, the conformation of Asp18 in the 18D/27D lysozyme (Fig. 2C, thick line) was different from that in the 18D/27N lysozyme (Fig. 2A, thick line). We considered that the side chain of Asp18 changed its position, allowing the amide group of Leu25 (N1) to form a hydrogen bond with WAT1, because of the

TABLE IV. **Distances between atoms involved in Ser24 (N-cap) in the B-helix of lysozymes.**

H-acceptor	H-donor	Distance (Å)			
		18N/27N	18D/27N (wild)	18N/27D	18D/27D
Asn27Nδ2	Ser24Oγ	2.73	2.94		
Ser24Oγ	Asp27Oδ1			2.83	2.65
Ser24Oγ	Asn/Asp27N	4.04[a]	4.08[a]	3.24	3.24
Ser24O	Trp28N	3.80[a]	3.74[a]	3.29	3.29

[a]The distance is too long for a hydrogen bond.

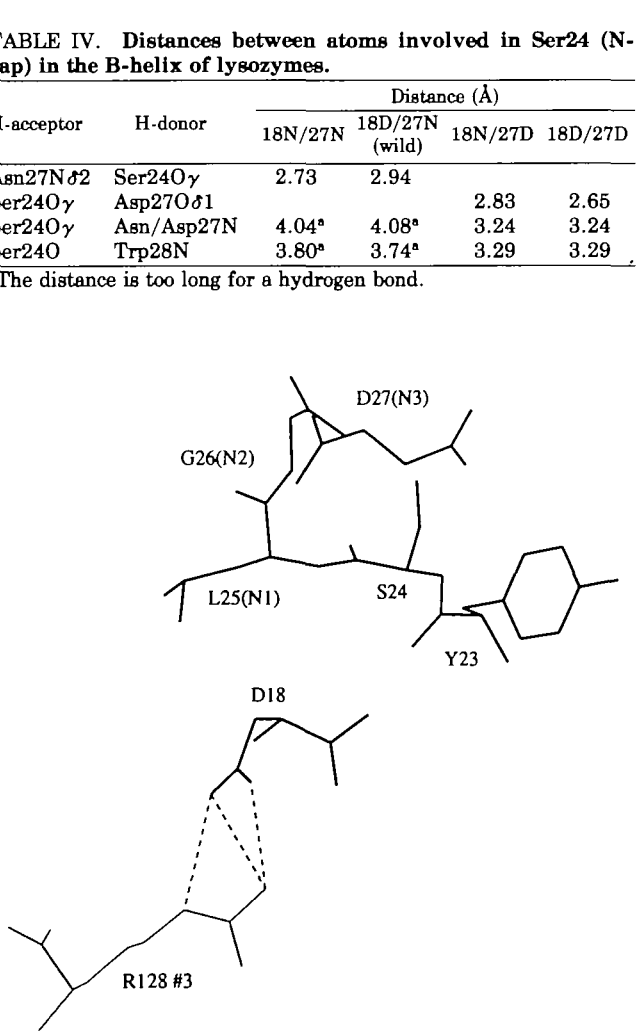

Fig. 3. **The crystal structure of the region near the N-terminus of the B-helix (25-35) in 18D/27D lysozyme (thick line).** The hydrogen bonds between the Asp18 side chain and the Arg128 side chain of a neighboring molecule (thin line) are shown.

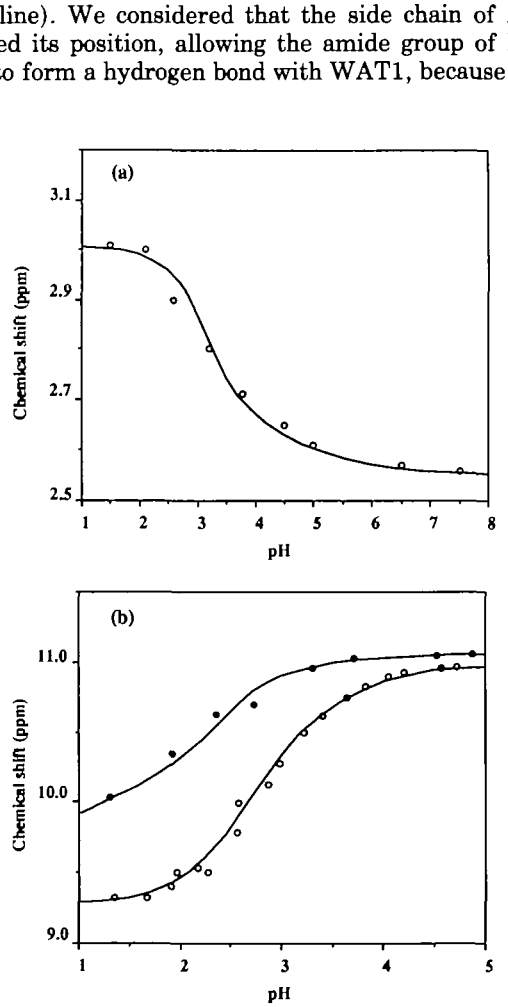

Fig. 4. **pH dependence of the chemical shifts of (a) the βCH proton of Asp18 in 18D/27D (open circles) lysozyme, and of (b) the indole proton of Trp111 in 18N/27D (closed circles) and 18D/27D (open circles) lysozymes.** Asp27 in both 18N/27D and 18D/27D lysozymes forms a hydrogen bond with the indole proton of Trp111.

TABLE V. **pK_a of Asp18 and Asp27 in lysozymes.**

	18N/27N	18D/27N (wild)	18N/27D	18D/27D
Asp18	–	2.3[a]	–	3.3
Asp27	–	–	<2.2	2.9

[a]The value is taken from Abe *et al.* (*17*).

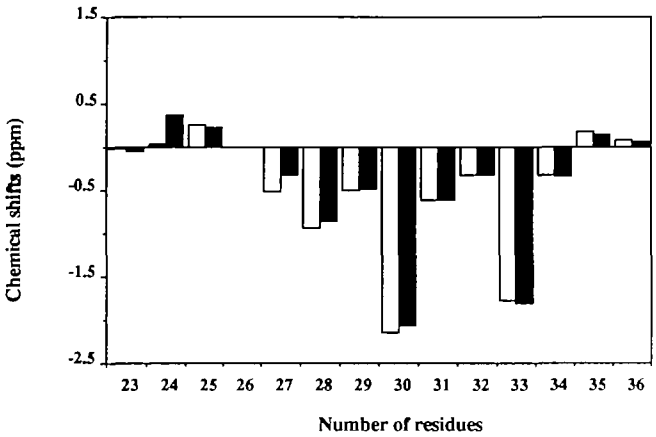

Fig. 5. **Chemical shift index of αCH in wild (open bar) and 18D/27D (closed bar) lysozymes at pH 3.8.**

electrostatic repulsion between Asp18 and Asp27 in the 18D/27D lysozyme. Figure 3 shows hydrogen bonds at Asp18 in the 18D/27D lysozyme. The hydrogen bonds are formed between the side chain of Asp18 and that of Arg128 in a neighboring molecule. This may be the result of the side chain at Asp18 having taken a different orientation in the 18D/27D lysozyme from that in the wild-type lysozyme.

pK_a Values of Asp18 and Asp27 in Mutant Lysozymes—To determine the pK_a values of Asp18 and Asp27, measurements of the 600 MHz ^{1}H-NMR spectra were conducted at 35°C and various pH values (1.5-7.5). The resonances of the Asp18 βCH and Trp111 indole protons were employed to follow the dissociation of Asp18 and Asp27 in each lysozyme, because Asp27 forms a hydrogen bond with the N-1 proton of Trp111 and because they were separated from other resonances. These resonances were assigned using the respective ^{1}H-^{1}H COSY and ^{1}H-^{1}H NOESY spectra. In Fig. 4, the measured chemical shifts are plotted against pH. The curve-fitting analysis was carried out for the pH dependence of the signal, and it was found that the pK_a values of Asp18 in the 18D/27N lysozyme (wild-type) was 2.3 (*17*), the pK_a of Asp27 in the 18N/27D lysozyme was below 2.2, and the pK_a of Asp18 and Asp27 in the 18D/27D lysozyme were 3.3 and 2.9, respectively (Table V). All pK_a values of Asp18 and Asp27 in the mutant lysozymes were lower than 4.0, which is the intrinsic value for the Asp residue. These results indicated that favorable electrostatic interactions were present at the positions of Asp18 and Asp27 in the wild-type and mutant lysozymes.

Analysis of B-Helix Structure by Two-Dimensional ^{1}H-NMR in 18D/27D Lysozyme—In order to analyze the secondary structure in solution around the B-helix in the 18D/27D lysozyme, which is the most stable lysozyme employed here, the assignments of the chemical shifts around the region in the mutant lysozyme were carried out.

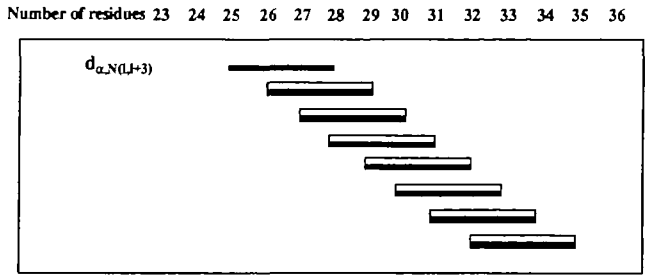

Fig. 6. **The NOE connectivities of 23-36 amino acid residues of wild (open bar) and 18D/27D (closed bar) lysozymes at pH 3.8.**

Those of the resonances in the wild-type lysozyme were taken from the literature (*16*). Figure 5 shows the chemical shift indexes of αCH in the wild-type and 18D/27D lysozymes at pH 3.8. The assignment of secondary structure was carried out according to the literature (*18*). The results indicated that Ser24 in the 18D/27D lysozyme has a β-conformation while that in the wild-type lysozyme does not. This is consistent with the results of the crystal structure determination. Figure 6 shows the NOE connectivities of 23-36 amino acid residues in the wild-type and 18D/27D lysozymes at pH 3.8. The NOE between αCH of Leu25 (N1) and NH of Trp28 (N4) was observed in the 18D/27D lysozyme, but not in the wild-type lysozyme.

DISCUSSION

We supposed that the negative charge at Asp18 contributes to stabilizing the wild-type lysozyme, because the pK_a of Asp18 was lower than the intrinsic pK_a of Asp from the NMR titration experiment on wild-type lysozyme using NMR (*17*). As was expected, the 18N/27N lysozyme was less stable than the wild-type (18D/27N) lysozyme. On the other hand, the 18D/27D and 18N/27D lysozymes were more stable than the 18N/27N lysozyme although the side chain of the residue at position 27 was less accessible to the solvent. This was confirmed by the finding that the pK_as of Asp27 in these mutant lysozymes were lower than the intrinsic pK_a of Asp (4.0). This seems strange because carboxyl groups on the inside of a protein molecule are hard to dissociate. For example, Glu35 in the lysozyme, which is located in the inside of lysozyme, has a higher pK_a (6.1) than the intrinsic value (*19*). From X-ray analysis, the dissociated side chain of Asp27 at the N3 position in the B-helix in these mutant lysozymes forms a hydrogen bond with Ser24 at the N-cap position on the B-helix. The NMR measurement of the 18D/27D lysozyme at pH 3.8 supported this X-ray result, indicating structural change around Ser24 with the appearance of a new NOE. Therefore, the side chain of Asp27 may be present in dissociated form under the conditions of X-ray crystallographic analysis (pH 4.7) and the conditions of the stability measurement (pH 5.5).

Zhukovsky *et al.* (*20*) demonstrated that a hydrogen bond between the side chain of the residue located at the N-cap position in the α-helix and the backbone of the residue located at the N3 position in the α-helix contributes to stabilizing a protein. However, in the wild-type (18D/27N) lysozyme, the interaction between the side chain at the N-cap position Ser24 and the backbone at N3 position

TABLE VI. **Distance and angle of hydrogen bond of amino group at the Leu25 residue (N1) in the B-helix of lysozymes.**

Lysozyme	H-acceptor	Distance	Angle[a]
18N/27N	WAT1O	2.98	165
18D/27N (wild)	Asp18Oε1	3.13	137
18N/27D	WAT1O	3.22	168
18D/27D	WAT1O	3.02	175

[a]The angle for amino to oxygen, *i.e.*, N—H···O.

Asn27 in the B-helix would not contribute to stabilizing the lysozyme because this distance is too long to form a hydrogen bond. On the other hand, in the 18N/27D and 18D/27D lysozymes, the distances between the side chain at the N-cap position Ser24 and the backbone at the N3 position Asp27 in the B-helix are short enough to allow hydrogen bond formation, due to the dissociation of aspartic acid at the N3 position (Asp27). From these results, we concluded that the favorable interactions in the N-terminus of the B-helix contributes to the increased stability of lysozymes with the dissociable Asp27.

The 18D/27D lysozyme was the most stable among the wild-type and mutant lysozymes. However, we wondered if the introduction of a new negative charge (Asp27) near the Asp18 may affect the dissociation of Asp18. This interaction would induce the structural change at the side chain of Asp18 in the 18D/27D lysozyme (Fig. 2C), allowing the side chain to hydrogen bond with Arg128 of the neighboring molecule (Fig. 3), and causing the pK_as of Asp18 and Asp27 in 18D/27D lysozyme to be higher than that of Asp18 in the wild-type (18D/27N) lysozyme and that of Asp27 in 18N/27D lysozyme (Table V). However, since the angle of the hydrogen bond of the amide group at the Leu25 residue in the wild-type (18D/27N) lysozyme was smaller than that in 18D/27D lysozyme, the hydrogen bond in the wild-type (18D/27N) lysozyme may be weaker than that in 18D/27D lysozyme (Table VI). From the structure and pK_a values of 18D/27D lysozyme, although an electrostatic repulsion between Asp18 and Asp27 residues in 18D/27D lysozyme was observed, the dissociation of each residue contributes to stabilizing the B-helix in 18D/27D lysozyme through hydrogen bonding and charge-helix macrodipole interaction. This is the first evidence that both of the two neighboring negative charges at the N-terminus of the helix both increase the stability of the protein. These results imply that these residues in rat, mouse P or mouse M lysozyme do contribute to the increased stability of the molecules.

The authors would like to thank Dr. T. Miki for his advice on gene engineering, Dr. T. Yamane of Nagoya University, Dr. Y. Hata of Kyoto University, Dr. R. Kuroki of Kirin Brewery Co., Ltd., and T. Shimizu of Nara Institute of Science and Technology for their advice in protein crystallography.

REFERENCES

1. Hol, W.G., van, Duijunen, P.T., and Berendsen, H.J. (1978) The α-helix dipole and the properties of protein. *Nature* **273**, 443-445
2. Richardson, J.S. and Richardson, D.C. (1988) Amino acid preferences for specific locations at the ends of helices. *Science* **240**, 1648-1652
3. Shoemaker, K.R., Kim, P.S., York, E.J., and Stewart, J.M. (1987) Tests of the helix dipole model for stabilization of α-helices. *Nature* **326**, 563-567
4. Sali, D., Bycroft, M., and Fersht, A.R. (1988) Stabilization of protein structure by interaction of α-helix dipole with a charged side chain. *Nature* **335**, 740-743
5. Sancho, J., Serrano, L., and Fersht, A.R. (1992) Histidine residues at the N- and C-termini of α-helices: Perturbed pK_as and protein stability. *Biochemistry* **31**, 2253-2258
6. Nicholson, H., Becktel, W.J., and Matthews, B.W. (1988) Enhanced protein thermostability from designed mutations that interact with α-helix dipoles. *Nature* **336**, 651-656
7. Walter, S., Hubner, B., Hahn, U., and Schmid, F.X. (1995) Destabilization of a protein helix by electrostatic interaction. *J. Mol. Biol.* **252**, 133-143
8. Hashimoto, Y., Yamada, K., Motoshima, H., Omura, T., Yamada, H., Yasukochi, T., Miki, T., Ueda, T., and Imoto, T. (1996) A mutant study of catalytic residue Asp52 in hen egg lysozyme. *J. Biochem.* **119**, 145-150
9. Inoue, M., Yamada, H., Yasukochi, T., Kuroki, R., Miki, T., Horiuchi, T., and Imoto, T. (1992) Multiple role of hydrophobicity of tryptophan-108 in chicken lysozyme: Structural stability, saccharide binding ability, and abnormal pK_a of glutamic acid-35. *Biochemistry* **31**, 5545-5553
10. Blake, C.C.F., Koenig, D.F., Mair, G.A., North, A.C.T., Phillips, D.C., and Sarma, V.R. (1965) Structure of hen lysozyme. A three-dimensional Fourier synthesis at 2 Å resolution. *Nature* **206**, 757-761
11. Brünger, A.T. (1991) Simulated annealing in crystallography. *Annu. Rev. Phys. Chem.* **42**, 197-223
12. Roussel, A., Fontecilla-Camps, J.C., and Cambillau, C. (1990) *TURBO-FRODO: A New Program for Protein Crystallography and Modeling*, Bordeaux, France: XV IUCr Congress
13. Bundi, A. and Wüthrich, K. (1983) ^{1}H NMR parameters of the common amino-acids residues measured in aqueous solution of the linear tetrapeptides H-Gly-Gly-X-Ala-OH. *Biopolymers* **18**, 285-297
14. Bodenhauser, H., Koger, H., and Ernst, R.R. (1984) Selection of coherence-transfer pathway in NMR pulse experiments. *J. Magn. Reson.* **58**, 370-388
15. Kumar, A., Ernst, R.R., and Wüthrich, K. (1980) A two-dimensional nuclear Overhauser enhancement (2D NOE) experiment for the elucidation of complete proton-proton cross-relaxation networks in biological macromolecules. *Biochem. Biophys. Res. Commun.* **95**, 1-6
16. Redfield, C. and Dobson, C.M. (1988) Sequential ^{1}H-NMR assignments and secondary structure of hen egg white lysozyme in solution. *Biochemistry* **27**, 122-136
17. Abe, Y., Ueda, T., Iwashita, H., Hashimoto, Y., Motoshima, H., Tanaka, Y., and Imoto, T. (1995) Effect of salt concentration on the pK_a of acidic residues in lysozyme. *J. Biochem.* **118**, 946-952
18. Wishart, D.S., Sykes, B.D., and Richard, F.M. (1992) The chemical shift: A fast and simple method for the assignment of protein secondary structure through NMR spectroscopy. *Biochemistry* **31**, 1647-1651
19. Imoto, T., Forster, L.S., Rupley, J.A., and Tanaka, F. (1972) Fluorescence of lysozyme: emissions from tryptophan residues 62 and 108 and energy migration. *Proc. Natl. Acad. Sci. USA* **69**, 1151-1155
20. Zhukovsky, E.A., Mulkerrin, M.G., and Presta, L.G. (1994) Contribution to global protein stabilization of the N-capping box in human growth hormone. *Biochemistry* **33**, 9856-9864
21. Imoto, T., Jonson, L.N., North, A.C.T., Phillips, D.C., and Rupley, J.A. (1972) Vertebrate lysozymes in *The Enzymes* (Boyer, P.D., ed.) Vol. 7, 3rd ed., pp. 665-868, Academic Press, New York
22. Canfield, R.E., Kammerman, S., Sobel, J.H., and Morgan, F.J. (1971) Primary structure of lysozymes from man and goose. *Nature New Biol.* **232**, 16-17
23. Cortopassi, G.A. and Wilson, A.C. (1990) Recent origin of the P lysozyme gene mice. *Nucleic Acids Res.* **18**, 1191
24. Cross, M., Mangelsdorf, I., Wedel, A., and Renkawitz, R. (1988) Mouse lysozyme M gene: isolation, characterization, and expression studies. *Proc. Natl. Acad. Sci. USA* **85**, 6232-6236
25. White, T.J., Mross, G.A., Osserman, E.F., and Wilson, A.C. (1977) Primary structure of rat lysozyme. *Biochemistry* **16**, 1430-1436